



HAL
open science

Temperature gradient based annealing methodology for tungsten recrystallization kinetics assessment

Maxime Lemetais, Matthieu Lenci, Claire Maurice, Timothée Devictor, Alan Durif, Marco Minissale, Marilyne Mondon, Gerald Pintsuk, David Piot, Laurent Gallais, et al.

► **To cite this version:**

Maxime Lemetais, Matthieu Lenci, Claire Maurice, Timothée Devictor, Alan Durif, et al.. Temperature gradient based annealing methodology for tungsten recrystallization kinetics assessment. *Fusion Engineering and Design*, 2023, 193, pp.113785. 10.1016/j.fusengdes.2023.113785 . emse-04102806

HAL Id: emse-04102806

<https://hal-emse.ccsd.cnrs.fr/emse-04102806>

Submitted on 31 May 2023

HAL is a multi-disciplinary open access archive for the deposit and dissemination of scientific research documents, whether they are published or not. The documents may come from teaching and research institutions in France or abroad, or from public or private research centers.

L'archive ouverte pluridisciplinaire **HAL**, est destinée au dépôt et à la diffusion de documents scientifiques de niveau recherche, publiés ou non, émanant des établissements d'enseignement et de recherche français ou étrangers, des laboratoires publics ou privés.

Temperature gradient based annealing methodology for tungsten recrystallization kinetics assessment

Maxime LEMETAIS^(a,b,c), Matthieu LENCI^(a), Claire MAURICE^(a), Timothée DEVICTOR^(a), Alan DURIF^(b), Marco MINISSALE^(e), Marilyne MONDON^(a), Gerald PINTSUK^(d), David PIOT^(a), Laurent GALLAIS^(c), Marianne RICHOU^(b), Guillaume KERMOUCHE^(a)

- (a) Mines Saint-Etienne, CNRS UMR 5307 LGF, Centre SMS, F – 42023 SAINT-ETIENNE CEDEX, France
- (b) CEA, IRFM, F-13108 SAINT-PAUL-LEZ-DURANCE, France
- (c) Aix-Marseille Univ, CNRS, Centrale Marseille, Institut Fresnel, MARSEILLE, France
- (d) Forschungszentrum Jülich GmbH, Institut für Energie- und Klimaforschung, 52425 JÜLICH, GERMANY
- (e) Aix-Marseille Univ, CNRS, PIIM, MARSEILLE, France

Keywords:

Characterization, high-temperature annealing, laser-based annealing, recrystallization, softening, tungsten, thermonuclear fusion, hardness

Abstract:

In future thermonuclear fusion reactors, like ITER and DEMO, plasma-facing components with tungsten armor material will have to sustain high thermal fluxes (10 MW/m² in steady state and 20 MW/m² in quasi-steady-state). For such extreme conditions, tungsten may reach temperatures higher than 1000 °C and, consequently can be prone to recrystallize, which can limit the lifetime of the divertor targets under cycling thermal loadings. Characterization of recrystallization kinetics involves the use of different methods and devices (furnace, laser heating) depending on the annealing temperature regime to be analyzed. For these methods, the heating and the subsequent characterisation of around 10 samples (5 × 4 × 4 mm) per annealing temperature is needed. In this article, a method is proposed to quantify the recrystallization kinetics between 1300 °C and 1600 °C using a limited number of samples and heating conditions. The basic idea is to induce a steady-state temperature gradient in tungsten rods by heating one side of the rod using a laser heating system. Tungsten rods (50 × 4 × 5 mm) were annealed with this method. The resulting microstructures are characterized using optical microscopy and hardness measurements. The different stages of tungsten softening are clearly evidenced. These first results can be considered as a proof of concept for the use of such a methodology to assess tungsten recrystallization at high temperature.

Introduction :

The nuclear fusion machines called “Tokamak” are studied for electricity production. This technology uses magnetic fields to confine particles. However, the confinement is not perfect so that the plasma facing components (PFCs) are heat loaded by convective heat transfer. One of the main challenges in building a nuclear fusion device is to design PFCs and related plasma facing materials (PFMs) that can withstand the extreme conditions existing during device operation. The divertor is the region where most of charged particles, driven by open magnetic field lines, heat load the lower part of the wall. Several zones composed the divertor region. The divertor target zone will have to cope with high particle flux up to 10²⁴ ions.m⁻².s⁻¹ [1] and high heat fluxes (up to 20 MW.m⁻²) [1]. Tungsten has been chosen as the PFM for the actively cooled PFCs in the divertor region of ITER [2], [3]. Indeed, amongst the many advantages that tungsten possesses, one could mention its high melting temperature point (3400 °C), low tritium retention and high thermal conductivity (175 W.m⁻¹.K⁻¹ at 20 °C). In the following, we will focus the study on the PFCs located in the ITER divertor target region. The technologies and manufacturing processes for these PFCs were qualified. During the qualification phase, which uses electron beam loading to mimic the PFCs thermal heat loading, macro-cracks have been reported after few thousands of cycles at 20 MW.m⁻² [4]. Those cracks may limit the lifetime of ITER PFCs [5]. These types of cracks are induced by the accumulation of plastic deformation during the thermal heat loading cycling of the PFCs [4], [5]. The plastic deformation is the consequence of the tungsten softening induced by high temperature field in tungsten. Indeed, when heat loaded at high temperature, tungsten microstructure changes (recovery and recrystallization) [6]–[8].

Assessment of softening and recrystallization is essential to predict the apparition of these particular macro-cracks. In the literature several methods are used, one of these is the experimental assessment of softening and recrystallization kinetics [9] after thermal annealing. With these kinetics, interpolation of softening and recrystallization processes may be deduced by adapted models [10], [11]. The tungsten microstructure after manufacturing have an impact of the studied kinetics [10]. For each manufacturing route, a full assessment of the softening/recrystallization kinetics required numerous annealing experiments (in the order of 10 for each annealing studied temperature)[10], [12], [13]. For conventional annealing experiment [9], [12], [13], one experiment corresponds to one annealing temperature and one annealing time. The assessment of the softening/recrystallization kinetics is realized by hardness and EBSD measurements.

In this paper, a gradient annealing method based on laser heating is proposed to reduce the number of annealing experiments to produce the softening recrystallization kinetics. The main idea is to prescribe a steady-state temperature gradient in the material by heating one of its faces with a laser. With this proposed method, one annealing experiment corresponds to the study of several annealing temperatures and one annealing time. After the thermal loading, softening is evaluated by measuring the hardness along the material induced thermal gradient. A qualitative assessment of this method is provided in this paper. In the first part of this paper, the method and the setup are presented in details. Then the method is applied to a tungsten material produced according to the ITER specifications. Results are used to quantify the softening kinetics using a JMAK law [8].

1. Annealing set-up

1.1. Principle

The studied annealing experiments have been conducted on the ChauCoLase (Chauffage Contrôlé par Laser) facility of institute Fresnel [9]. The laser used is a high power continuous wave Ytterbium fiber laser (SPI laser Qube 1500) emitting at a wavelength of 1080 nm [9]. This laser can deliver a maximum power of 1500 W with a monomode laser beam and a typical rising time of few microseconds [9]. The basic idea of the gradient annealing treatment is to induce a steady-state temperature gradient along the rod by heating one face of the sample and to investigate temperatures from 1200 °C and 2400 °C. Steady-state thermal regime is obtained when radiation losses and laser radiation absorption are in balance. Finite element modeling (FEM) is used to define the adapted sample geometry and power load to reach steady-state temperature gradients within the rod (Figure 1). The studied sample is a rod with a section of 4×5 mm and a length of 50 mm. In FEM simulation, laser input heat flux is represented by a Gaussian profile on the face heated by the laser with a power of 200 W. Heat is released by thermal radiation from all the surfaces (Figure 1a). The FEM software COMSOL is used to resolve the heat equation in solid for conduction regime [9]. Thermal conductivity, thermal capacity, density, and emissivity values in the model depends on the temperature according to ITER Material Properties Handbook. The simulated temperature is shown in Figure 1b. The temperature ranges between 1200 °C to 2400 °C along the rod length. Within the sections parallel to the surface heated by the laser, a temperature gradient is also present (Figure 1c). The maximal difference between the center and the corner of each sections does not exceed 4°C. For this reason, sections are considered isothermal. The laser power and studied sample dimensions fit to the thermal gradient requirement so that the heating conditions and sample dimension (4 × 5 × 50 mm) are set.

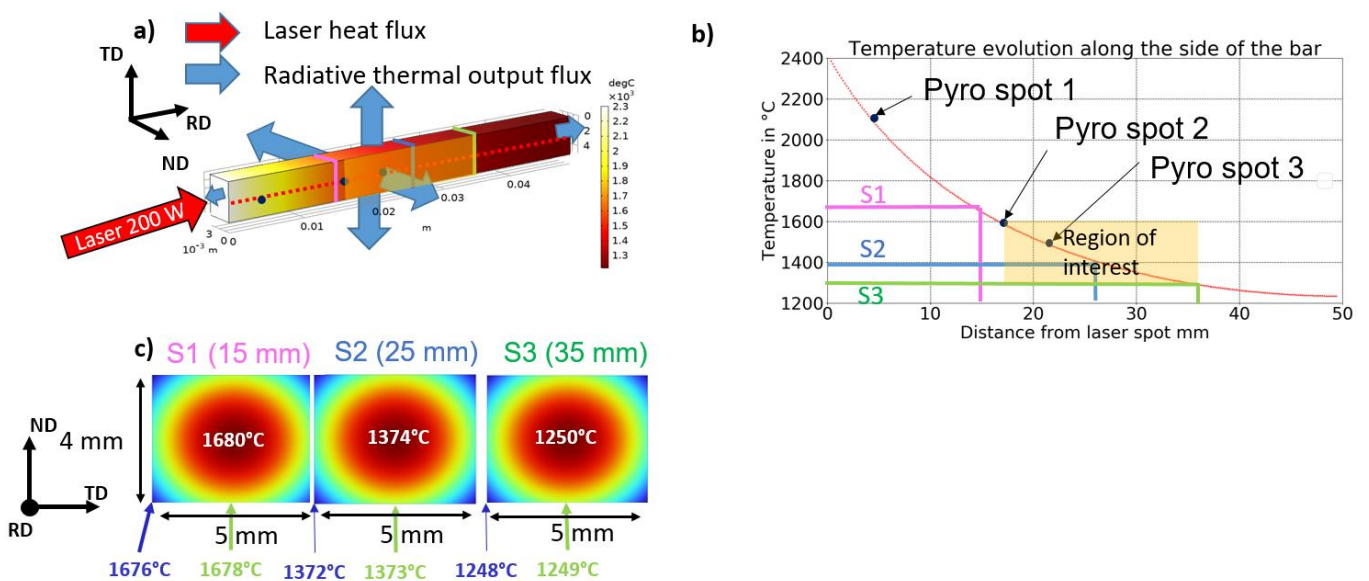


Figure 1.a) Thermal input and output fluxes represented by red and blue arrows. Temperature of the rod ranges between 1200 °C and 2400 °C along the RD axis. Temperature profile is computed by finite element with COMSOL Multiphysics software (red line) on the (RD, TD) surface. Region where transition from raw to recrystallized material is expected is highlighted in orange. b) Simulated temperature along the RD axis (in red computed by COMSOL Multiphysics) and measured temperatures with the 3 pyrometers according to the experimental set-up described in section II.1 c) Temperature field in sections (TD,ND) (S1, S2, S3) respectively located at 15, 25, and 35 mm from the laser heated spot. Red zone in the center corresponds to the highest temperature and blue zone on the corners corresponds to lowest temperature.

1.2. Studied material

One tungsten material, hot rolled along two perpendicular directions is investigated [14]. Samples are cut out from 225×225×12 mm plates by electro-discharge machining (EDM) process. Sample dimensions are 50×4×5 mm. The longest dimension (50 mm) is parallel to the rolling directions (RD). The shortest direction (4 mm) is parallel to the normal direction (ND) (Figure 2). Polishing is required to ensure a smooth and well-controlled surface finish for pyrometric measurements. The samples were mechanically polished with Silicon Carbide abrasive grinding papers from P200 to P1200 and then by diamond suspension of 3 μm and 1 μm before annealing.

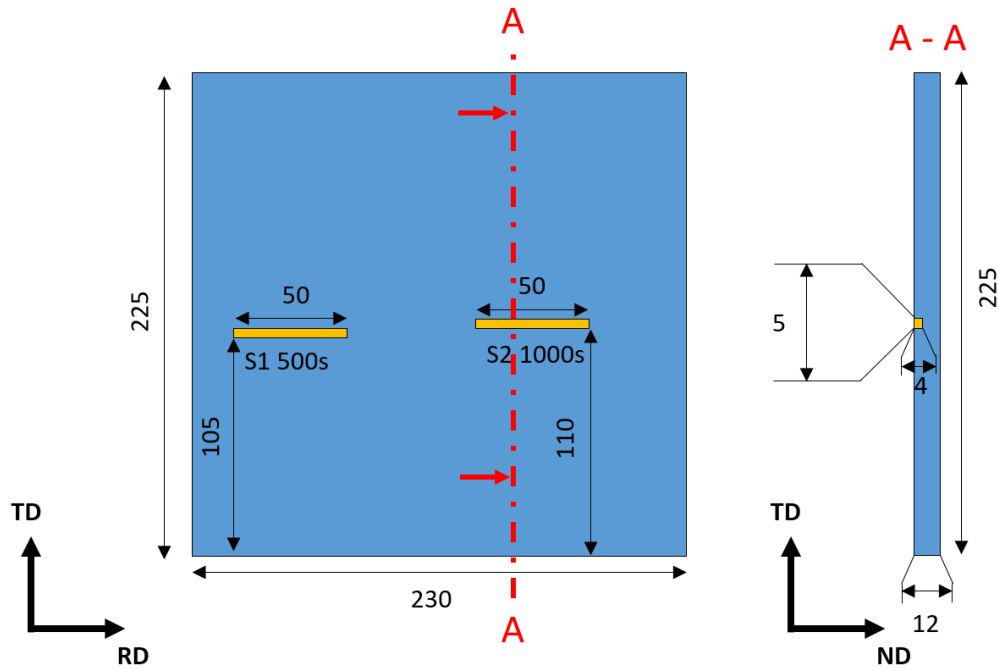


Figure 2. The sample are rods (in orange) extracted from a hot rolled tungsten plate (in blue). The rod sample dimensions are $5 \times 4 \times 50$ mm. The rod was extracted from the skin to $1/3$ of the thickness of the plate. Dimensions are indicated in mm. RD corresponds to the first rolling axis, TD corresponds to the second rolling axis and ND corresponds to the axis normal to the rolling directions.

I.3 Post-mortem characterization

After annealing, Vickers hardness measurements (10 kg) are performed on the surface containing the rolling directions (RD, TD). Staggered row pattern is used to maximize the number of measurements on the surface studied. In order to avoid overlapping between the plastic zones of imprints, the distance between two indentation centers is greater than 2.5 diagonals of these indentations to comply with the American Society for Testing and Materials (ASTM) international standard [15]. Two imprints on different staggered rows are spaced from $750 \mu\text{m}$. On a same line, the distance between two imprints is around $1000 \mu\text{m}$.

2. Results and discussions

2.1. Upgrade of the experimental set-up (heat loading and hardness assessment)

The high power laser-based heating set-up, presented in Figure 3a) and described in details in [9] is upgraded to apply the thermal annealing conditions. One part of this upgrade consists, during annealing, to regulate the laser power through a feedback loop by controlling the temperature located at 5 mm from the laser spot thanks to a pyrometer (Pyro spot 1 on Figure 3b and c). To reach the steady-state thermal condition, the increases with a heating speed of $15 \text{ }^\circ\text{C/s}$ (measured at the Pyro spot 1) is applied. The heating speed value results of a compromise between getting as fast as possible to the steady-state regime and minimizing the temperature overshoot ($\sim 6 \text{ }^\circ\text{C}$). The impact of the heating speed will be studied in the future. Once the prescribed temperature at the Pyro spot 1 is reached, the temperature is maintained during few hundreds of seconds. Two other pyrometers (Pyro spot 2 and Pyro spot 3 on Figure 3b and c) are used to identify the position of the isothermal surface corresponding to temperatures around $1600 \text{ }^\circ\text{C}$ and $1500 \text{ }^\circ\text{C}$ respectively. The pyrometers 1, 2 and 3 are monochromatic pyrometers designed for tungsten (wavelength of $1.27 \mu\text{m}$) on a temperature range going from $600 \text{ }^\circ\text{C}$ to $3000 \text{ }^\circ\text{C}$. Temperatures estimated by the simulation (input power = 200 W) are in line with those measured by the pyrometers (Figure 1b).

Hardness is evaluated from the calculation of the mean values (\overline{HV}) obtained from both diagonals of four imprints located in the softening region at a supposed equal distance from the surface heated by laser (blue inset Figure 4). The corresponding temperature is assessed by the results of the FEM. A small deviation of imprint position along the RD axis can be observed between the four imprints of a same column (Figure 4).

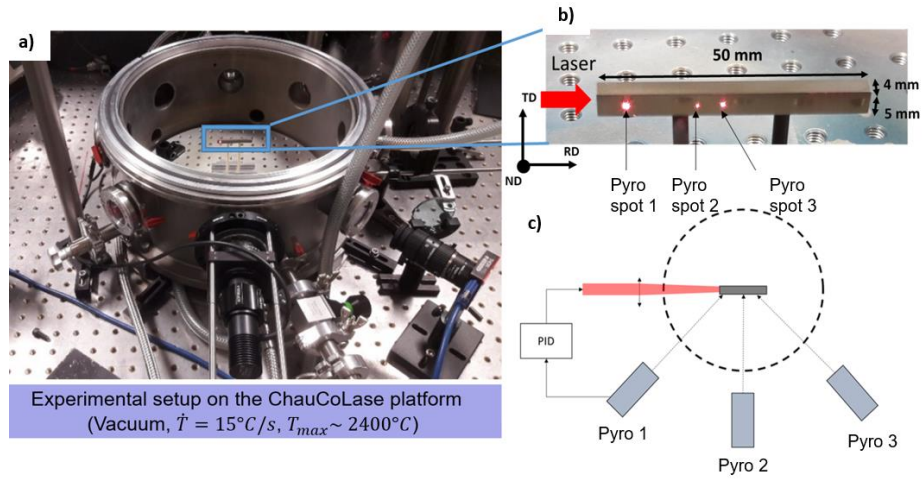


Figure 3. a) Vacuum chamber of the ChauCoLase set-up with one rod enclosed. b) Picture and dimensions of the rod. Three positions where the temperature are measured by the pyrometers are highlighted in red on the tungsten rod. c) Diagram of the ChauCoLase set-up where the three pyrometers are shown. Pyro 1 is used to regulate the input power thanks to a PID controller.

2.2. Softening – Effect of annealing time

Two rods were annealed with this method. One with the annealing temperature of 500s and the other one with the annealing temperature of 1000 s. Pictures of imprints are shown on Figure 4. Grain boundaries revealed by thermal etching can be observed in Figure 4. Thermal etching is induced by diffusion and evaporation, which create grooves on the surface of the material at grain boundaries location. This phenomenon appears during annealing at high temperature in an inert atmosphere. Thermal etching appears in black on the picture of imprints shown in Figure 4. Above 1600 °C, the diagonal extremities are consequently difficult to determine. Standard deviation on temperature is obtained by FEM simulations. It is estimated from the temperature variation corresponding to the variation of position of the four imprints considered for the hardness assessment (Figure 4.). Standard deviations on the temperature obtained by FEM simulations does not exceed 3 °C. Standard deviation on hardness is the standard deviation obtained from the hardness measurement, corresponding to the group of four imprints located at an equal distance from the laser. Standard deviation on hardness does not exceed 13 HV. For both samples, the softening front (hardness decrease) is observed between 20 mm and 35 mm corresponding to temperatures ranging from 1500 °C and 1300 °C respectively (Figure 4).

Hardness and simulated temperature profile are plotted in Figure 5. For the sample heated during 1000 s the hardness curve is shifted to a position farther on the RD axis. This is consistent with the fact that, for a given temperature, softening is higher for a higher annealing time.

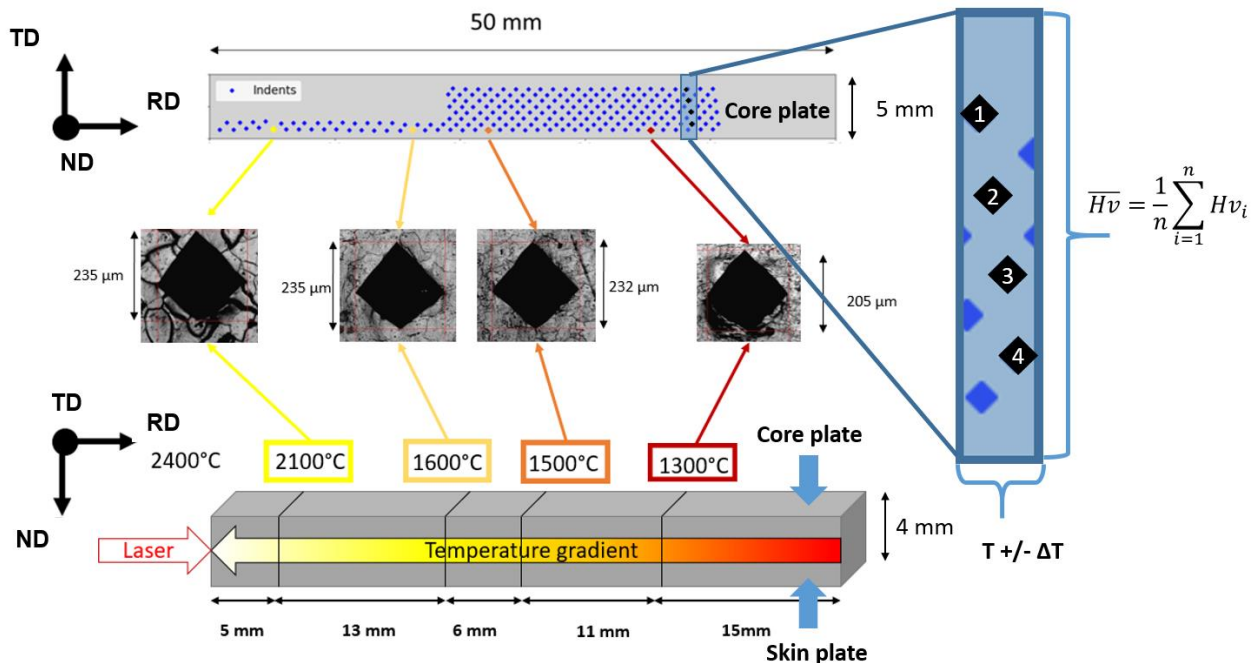


Figure 4. The sketch at the top gives an indentation pattern grid and imprint along the sample annealed for 1000 s. Hardness (\overline{HV}) is computed from the mean diagonals of imprints located at a same distance from the heated surface (H_i). On the figure, 4 imprints ($n=4$) are taken for the hardness calculation (\overline{HV}). The sketch at the bottom gives the correlation between the locations and temperatures obtained from the modelling. At the center of the figure, pictures of imprints made at different distance of the laser are given.

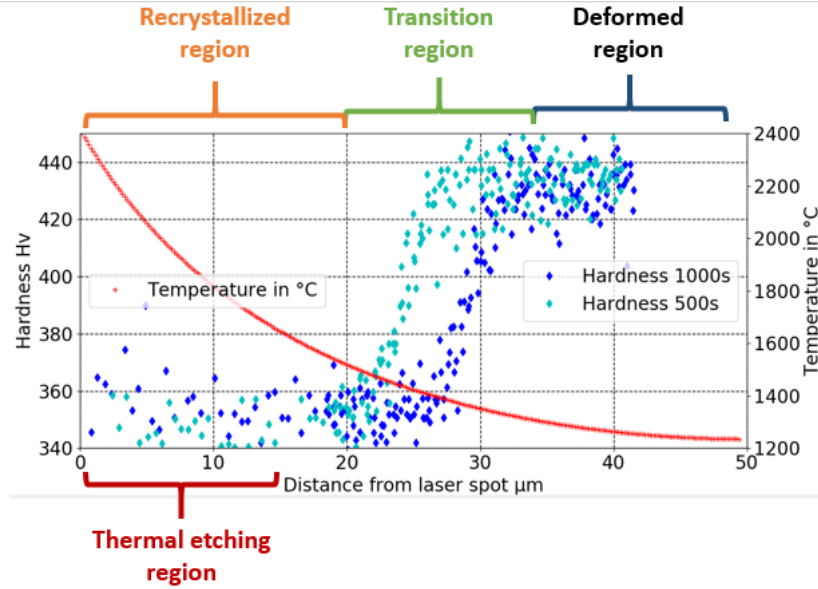


Figure 5. Evolution of hardness measurement and simulated temperature of two annealed rods (500s and 1000s). Hardness data for the sample annealed during 1000 s is plotted in dark blue. Hardness data for the sample annealed during 500 s is plotted in cyan. The red line corresponds to the simulated temperature along the rod. Three region are identified for each rod from left to right: a first region where the hardness corresponds to the recrystallized materia.(Close to the laser, hardness measurement spreading is higher due to thermal etching). A second region where hardness evolves from the hardness of the softened material to a higher hardness corresponding to the hardness of the material prior to annealing and a third region where hardness corresponds to the hardness of the material before annealing.

2.3. Assessment of softening kinetics with Johnson-Mehl-Avrami-Kolmogorov (JMAK) model

In this paper, the recrystallization kinetics is considered to be roughly equivalent to the softening kinetics. It is quantified through the use of a JMAK model (Equation 1) [10], [16].

$$X_H = 1 - \exp(-kt^n) \quad \text{Equation 1} \quad (1)$$

where X_H is the softening fraction, n is the JMAK exponent and k is a temperature dependent parameter given by Equation 2

$$k = \ln(2) \times \left[C \times \exp\left(\frac{-Q}{RT}\right) \right]^n \quad \text{Equation 2} \quad (2)$$

Q is the activation energy for recrystallization and C is a frequency constant. Quantification of recrystallization kinetics requires the estimation of n , C and Q parameters. The evolution of softening fraction X_H along the rod is estimated from the Equation 3.

$$X_H = \frac{\overline{HV} - HV_{rex}}{HV_{def} - HV_{rex}} \quad \text{Equation 3} \quad (3)$$

where HV_{def} is the initial tungsten hardness (after rolling step), HV_{rex} is the hardness of fully recrystallized tungsten and \overline{HV} is the mean value of hardness (Figure 5).

The imprints in the thermally etched region (above 1600 °C) are not taken into account for the computation of the mean hardness in the softened area (HV_{rex}). HV_{rex} , is estimated from the mean value of the hardness of the imprints situated between 1500 °C and 1600 °C, where softening is supposed to be complete (Figure 5). The recrystallized hardness measured in this zone is 350 ± 8 HV for the sample annealed during 500 s (S500s) and 354 ± 7 HV for the sample annealed during 1000 s (S1000s). Those values are consistent with those reported in the literature [11][12][13].

HV_{def} is estimated from the hardness in the deformed zone (< 1300 °C). HV_{def} measured on the sample annealed during 500 s (resp. 1000s) is equal to 434 ± 7 HV (resp. 430 ± 9 HV). In comparison, the mean hardness measured on the initial tungsten plate core before annealing is 432 ± 6 HV.

The softening fraction is plotted as a function of temperature for a given annealing time (Figure 6). The JMAK parameters are assessed. n (Equation 1) can be estimated from the shape of the curves (softening transition slope steepness). k can be estimated from the Arrhenius law at half-recrystallization ($X_H = 0.5$). Q and C are estimated by minimizing the errors between experimental and numerical results using a least square method. The JMAK resulting model is enclosed in Figure 6. One can see a good adjustment of the model with regard to the experimental data. Estimated activation energy Q (224 kJ/mol) seems to be low compared to those reported in literature, these later being assessed at a lower temperature [11]–[13]. This might be the consequence of a high temperature regime for recrystallization in tungsten that would differ from the low temperature one. The competition between recovery and recrystallization might be different at a higher temperature. To assess such a conclusion, which would be of primary importance to predict PFC lifetime, additional laser-based annealing experiments and complementary microstructural

characterizations (EBSD, nanoindentation [22]) are required. Standard deviation associated to the softening fraction corresponds to the error bar associated with each points on Figure 6.

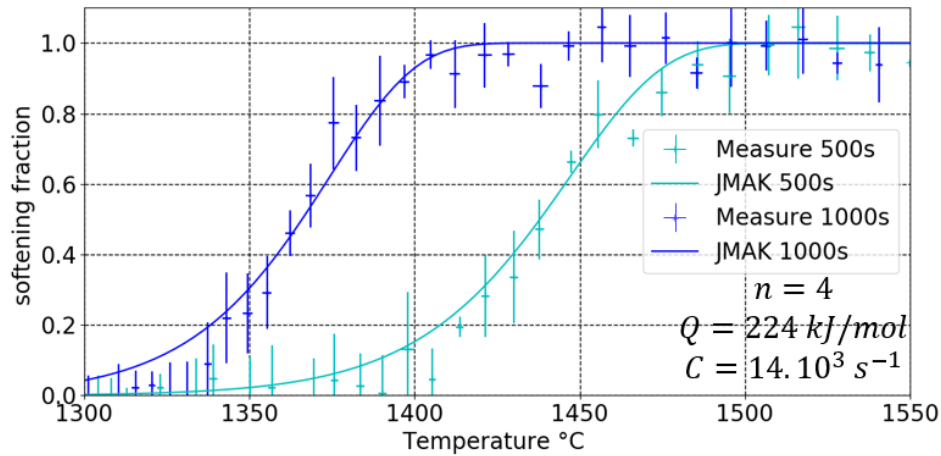


Figure 6. Softening fraction as a function of annealing temperature assessed experimentally for two annealed times (500s, 1000s). Corresponding JMAK model is plotted for the two annealed times

Conclusions and perspectives

A novel laser-based annealing gradient method has been presented in this paper. With this proposed method, one annealing experiment corresponds to the study of several annealing temperatures and one annealing time. The principle is to produce a temperature gradient within the material, machined as a rod, by heating one face of the sample with a laser. Finite element modeling (FEM) is used to define the adapted rod geometry and the power load to reach, in steady state, the temperature gradient (1200°C – 2400°C) within the rod. The temperature gradient estimated by the simulation is in line with the measured one. After the thermal loading, softening is evaluated by measuring the hardness along the rod. The annealed temperature corresponding to the measured hardness is assessed by FEM. The drop of hardness within the rod and its position within the rod are consistent with the temperature profile in the tungsten rod. Softening occurs at lower temperature when annealing time is higher. A JMAK model is fitted on the experimental data. With these results, the temperature gradient based annealing methodology is considered qualitatively validated. To validate the method quantitatively, the proposed annealing method should be compared to conventional laser-based annealing method [10] using similar materials and annealing conditions .

Acknowledgement

This work has been carried out within the framework of the EUROfusion Consortium, funded by the European Union via the Euratom Research and Training Programme (Grant Agreement No 101052200 — EUROfusion). Views and opinions expressed are however those of the author(s) only and do not necessarily reflect those of the European Union or the European Commission. Neither the European Union nor the European Commission can be held responsible for them.

Bibliography

- [1] H. Bolt *et al.*, « Plasma facing and high heat flux materials – needs for ITER and beyond », *Journal of Nuclear Materials*, vol. 307-311, p. 43-52, déc. 2002, doi: 10.1016/S0022-3115(02)01175-3.
- [2] T. Hirai *et al.*, « Status of technology R&D for the ITER tungsten divertor monoblock », *Journal of Nuclear Materials*, vol. 463, p. 1248-1251, août 2015, doi: 10.1016/j.jnucmat.2014.12.027.
- [3] D. Acker *et al.*, « ITER PLASMA FACING COMPONENTS IAEA, VIENNA, 1991 IAEA/ITER/DS/30 », p. 145.
- [4] R. A. Pitts *et al.*, « Physics basis for the first ITER tungsten divertor », *Nuclear Materials and Energy*, vol. 20, p. 100696, août 2019, doi: 10.1016/j.nme.2019.100696.
- [5] G. Pintsuk *et al.*, « Characterization of ITER tungsten qualification mock-ups exposed to high cyclic thermal loads », *Fusion Engineering and Design*, vol. 98-99, p. 1384-1388, oct. 2015, doi: 10.1016/j.fusengdes.2015.01.037.
- [6] A. Durif, M. Richou, G. Kermouche, M. Lenci, et J.-M. Bergheau, « Impact of tungsten recrystallization on ITER-like components for lifetime estimation », *Fusion Engineering and Design*, vol. 138, p. 247-253, 2019, doi: 10.1016/j.fusengdes.2018.11.003.
- [7] S. Panayotis *et al.*, « Self-castellation of tungsten monoblock under high heat flux loading and impact of material properties », *Nuclear Materials and Energy*, vol. 12, p. 200-204, août 2017, doi: 10.1016/j.nme.2016.10.025.
- [8] A. Durif, M. Richou, G. Kermouche, et J.-M. Bergheau, « Inverse identification of tungsten static recrystallization kinetics under high thermal flux », *Fusion Engineering and Design*, vol. 146, p. 1759-1763, sept. 2019, doi: 10.1016/j.fusengdes.2019.02.141.
- [9] M. Minissale *et al.*, « A high power laser facility to conduct annealing tests at high temperature », *Review of Scientific Instruments*, vol. 91, n° 3, p. 035102, mars 2020, doi: 10.1063/1.5133741.
- [10] M. Richou *et al.*, « Recrystallization at high temperature of two tungsten materials complying with the ITER specifications », *Journal of Nuclear Materials*, vol. 542, p. 152418, déc. 2020, doi: 10.1016/j.jnucmat.2020.152418.
- [11] A. Durif *et al.*, « Competition between recovery and recrystallization in two tungsten supplies according to ITER specifications », *J Mater Sci*, vol. 57, n° 15, p. 7729-7746, avr. 2022, doi: 10.1007/s10853-022-07123-w.

- [12] A. Alfonso, D. Juul Jensen, G.-N. Luo, et W. Pantleon, « Recrystallization kinetics of warm-rolled tungsten in the temperature range 1150–1350°C », *Journal of Nuclear Materials*, vol. 455, n° 1, p. 591-594, déc. 2014, doi: 10.1016/j.jnucmat.2014.08.037.
- [13] A. Alfonso, D. Juul Jensen, G.-N. Luo, et W. Pantleon, « Thermal stability of a highly-deformed warm-rolled tungsten plate in the temperature range 1100–1250°C », *Fusion Engineering and Design*, vol. 98-99, p. 1924-1928, oct. 2015, doi: 10.1016/j.fusengdes.2015.05.043.
- [14] J.-H. Yu, H. Tanigawa, D. Hamaguchi, et T. Nozawa, « Mechanical properties of three kinds of ITER-Grade pure tungsten with different manufacturing processes », *Fusion Engineering and Design*, vol. 157, p. 111679, août 2020, doi: 10.1016/j.fusengdes.2020.111679.
- [15] E04 Committee, « Test Method for Microindentation Hardness of Materials », ASTM International. doi: 10.1520/E0384-17.
- [16] « Recrystallization and Related Annealing Phenomena - 1st Edition ». <https://www.elsevier.com/books/recrystallization-and-related-annealing-phenomena/humphreys/978-0-08-041884-1> (consulté le 16 juin 2022).